

# The induced $\Lambda\bar{\Lambda}$ and $\Xi^-\bar{\Xi}^+$ decay modes of the $Y(4220)$ as a vector charmonium

Ri-Qing Qian<sup>1,2,\*</sup>, Qi Huang<sup>4,†</sup> and Xiang Liu<sup>1,2,3,§</sup>

<sup>1</sup>*School of Physical Science and Technology, Lanzhou University, Lanzhou 730000, China*

<sup>2</sup>*Research Center for Hadron and CSR Physics, Lanzhou University & Institute of Modern Physics of CAS, Lanzhou 730000, China*

<sup>3</sup>*Lanzhou Center for Theoretical Physics, Key Laboratory of Theoretical Physics of Gansu Province, and Frontiers Science Center for Rare Isotopes, Lanzhou University, Lanzhou 730000, China*

<sup>4</sup>*School of Physical Sciences, University of Chinese Academy of Sciences (UCAS), Beijing 100049, China*

(Dated: November 30, 2021)

In this work, we explore the decay channels  $Y(4220) \rightarrow \Lambda\bar{\Lambda}$  and  $\Xi^-\bar{\Xi}^+$  by treating the  $Y(4220)$  as a vector charmonium state. The possible signals of the  $Y(4220)$  in the  $\Lambda\bar{\Lambda}$  and  $\Xi^-\bar{\Xi}^+$  channels are pointed out. Based on the hadronic loop mechanism, the extracted branching ratios of the  $Y(4220) \rightarrow \Lambda\bar{\Lambda}$  and  $\Xi^-\bar{\Xi}^+$  processes are reproduced, and the ratio and phase of the time-like electromagnetic form factors (EMFFs) are predicted. For the EMFFs of  $\Lambda$  at  $\sqrt{s} = m_{Y(4220)}$ ,  $|G_E^\Lambda/G_M^\Lambda|$  and  $\Delta\Phi^\Lambda$  are predicted to be  $|G_E^\Lambda/G_M^\Lambda| = 2.36$  and  $\Delta\Phi^\Lambda = 2.74^\circ$ , and those of  $\Xi^-$  are predicted to be  $|G_E^{\Xi^-}/G_M^{\Xi^-}| = 0.40$  and  $\Delta\Phi^{\Xi^-} = -115.60^\circ$ . These predictions can be treated as tests for the charmonium assignment of the  $Y(4220)$ .

## I. INTRODUCTION

Although more and more charmonia have been observed since 1974 [1, 2], it is not the end of the story of constructing the charmonium family, especially with a series of observations of charmoniumlike  $XYZ$  states [3, 4]. As an important group, the charmonium family may provide crucial hints when quantitatively depicting the interaction between quarks, which has close relation to the color confinement in Quantum Chromodynamics.

The vector charmoniumlike  $Y$  state around 4.2 GeV plays a special role in constructing the charmonium family. In 2014, the Lanzhou group predicted the existence of a vector charmonium  $\psi(4S)$  by borrowing the similarity between  $J/\psi$  and  $\Upsilon$  families [5]. In Ref. [5], the mass of the predicted  $\psi(4S)$  is 4263 MeV, which is consistent with former prediction of  $\psi(4S)$  by the screening potential model [7]. Obviously, this study proposed a new task for the future experiments at that time. As indicated in Ref. [8], a possible enhancement structure around 4.2 GeV may exist in the experimental data of the  $e^+e^- \rightarrow h_c\pi^+\pi^-$  [9] and the  $e^+e^- \rightarrow J/\psi\pi^+\pi^-$  [10] processes, which should be checked by more precise experimental studies. In 2015, the BESIII Collaboration analyzed the  $e^+e^- \rightarrow \chi_{c0}\omega$  process [11], where an obvious enhancement structure with mass  $M = 4230 \pm 8$  MeV and width  $\Gamma = 38 \pm 12$  MeV was found. Focusing on this novel phenomenon, the Lanzhou group indicated that this enhancement around 4.2 GeV in the  $\chi_{c0}\omega$  invariant mass spectrum can be understood through introducing the predicted  $\psi(4S)$  [12]. Also, in Ref. [13], the Lanzhou group found the evidence of  $\psi(4S)$  in the  $e^+e^- \rightarrow \psi(2S)\pi^+\pi^-$  data reported by the Belle Collaboration [15], where the extracted resonance parameters are  $M = 4243 \pm 7$  MeV and  $\Gamma = 16 \pm 31$  MeV. Additionally, by performing a combined fit to the  $e^+e^- \rightarrow \psi(2S)\pi^+\pi^-$

[15],  $h_c\pi^+\pi^-$  [9] and  $\chi_{c0}\omega$  [16] processes, similar resonance parameters were obtained for the narrow structure around 4.2 GeV [13]. In 2017, the BESIII Collaboration studied the  $e^+e^- \rightarrow \psi(2S)\pi^+\pi^-$  process based on  $5.1 \text{ fb}^{-1}$  of data [17] and confirmed the existence of the charmoniumlike structure around 4.2 GeV in the  $\psi(2S)\pi^+\pi^-$  invariant mass spectrum predicted by the Lanzhou group. Besides these studies of hidden-charm decays, BESIII found the evidence of a structure in the  $e^+e^- \rightarrow \pi^+D^0D^{*-}$  reaction around 4.2 GeV [18]. Focusing on these phenomena of the vector charmoniumlike structure around 4.2 GeV, further study from the Lanzhou group indicated that this structure plays a role of scaling point when constructing the  $J/\psi$  family [19], where the assignment of the mixture state of  $\psi(4S)$  and  $\psi(3D)$  to the vector charmoniumlike structure around 4.2 GeV was proposed to describe the present experimental data [15, 16, 18, 20, 21]. By this brief review, we retrospect the research status around these phenomena of the vector charmoniumlike structure at 4.2 GeV. In the following work, the vector charmoniumlike structure at 4.2 GeV is referred to as the  $Y(4220)$ .

To further clarify the properties of the  $Y(4220)$ , it is important to explore more decay channels of the  $Y(4220)$  in both theoretical and experimental aspects. Besides the open charm decay channels of the  $Y(4220)$ , the hidden charm decays and light-hadron decays of the  $Y(4220)$  can also provide important information. Recently, we noticed that measurements on the cross sections of the  $e^+e^- \rightarrow \Lambda\bar{\Lambda}$  [23] and  $e^+e^- \rightarrow \Xi^-\bar{\Xi}^+$  channels were given by the BESIII Collaboration [24]. When checking the experimental data, we find that there exists possible event accumulation around 4.2 GeV in the  $\Lambda\bar{\Lambda}$  and  $\Xi^-\bar{\Xi}^+$  invariant mass spectrum. Thus, it is a good opportunity to explore the  $\Lambda\bar{\Lambda}$  and  $\Xi^-\bar{\Xi}^+$  decay channels of the  $Y(4220)$ .

There is another reason for us to carry out this study. Recently, several measurements on the time-like electromagnetic form factors (EMFFs) of the hyperons have been done. For example, the EMFFs of  $\Lambda$  were measured at  $\sqrt{s} = m_{J/\psi}$  [22] and  $\sqrt{s} = 2.396$  GeV [25], the EMFFs of  $\Xi^-$  were obtained at  $\sqrt{s} = m_{J/\psi}$  [26], the EMFFs of  $\Sigma^+$  were measured at  $\sqrt{s} = m_{J/\psi}$  and  $\sqrt{s} = m_{\psi'}$  [27]. In these experiments, both module and phase of EMFFs were extracted via the subsequent decay of the hyperons. We should point out that at

\*Corresponding author

<sup>\*</sup>Electronic address: qianrq18@lzu.edu.cn

<sup>†</sup>Electronic address: huangqi@ucas.ac.cn

<sup>§</sup>Electronic address: xiangliu@lzu.edu.cn

specific resonance point such as  $\sqrt{s} = m_{J/\psi}$ , these EMFFs actually provide a complete measurement of the amplitude of resonance decay, and the properties of the resonance can be inferred from the EMFFs. Hence, the hyperon anti-hyperon pairs serves as special decay modes of vector charmonium states.

In this work, we explore the  $\Lambda\bar{\Lambda}$  and  $\Xi^-\bar{\Xi}^+$  decay channels of the  $Y(4220)$  under the assumption that the  $Y(4220)$  is a vector charmonium state. We relate the EMFFs of  $\Lambda$  and  $\Xi^-$  at  $\sqrt{s} = m_{Y(4220)}$  to the decays of  $Y(4220) \rightarrow \Lambda\bar{\Lambda}$  and  $\Xi^-\bar{\Xi}^+$  under the hadronic loop mechanism. Based on this point, the EMFFs of  $\Lambda$  and  $\Xi^-$  at  $\sqrt{s} = m_{Y(4220)}$  are predicted.

This paper is organized as follow. Firstly, we introduce the formalism used to discuss the  $\Lambda\bar{\Lambda}$  and  $\Xi^-\bar{\Xi}^+$  decay modes of the  $Y(4220)$  in Sec. II, where the hadronic loop mechanism in these decay channels is introduced in Sec. II A and their relation to the EMFFs of  $\Lambda$  and  $\Xi^-$  at  $\sqrt{s} = m_{Y(4220)}$  is discussed in Sec. II B. Then, the numerical results and discussions are present in Sec. III. Finally, this paper ends with the discussion and conclusion.

## II. THEORETICAL FORMALISM

### A. The decay process $Y(4220) \rightarrow \Lambda\bar{\Lambda}$ and $\Xi^-\bar{\Xi}^+$ under the hadronic loop mechanism

In Ref. [19], it was pointed out that the  $Y(4220)$  can be a good candidate of charmonium state. Thus in this section, assigning the  $Y(4220)$  to be a charmonium state, we investigate its decay into hyperon and antihyperon. Generally, these higher charmonia above the  $D\bar{D}$  threshold have dominant open-charm decay channel, which contributes to their total decay widths. Since the coupled-channel effect may play important role to mediate the decays of higher charmonia, we should consider the hadronic loop contribution to the decay channels involved in light hadrons for these discussed higher charmonia. Similar ideas have been successfully applied to the exploration of the hidden-charm and hidden-bottom decay of charmonia and bottomonia [28–41]. Obviously, the reported  $Y(4220)$  is a typical higher charmonium above the  $D\bar{D}$  threshold. In this work, we study the hadronic loop effect to the processes  $Y(4220) \rightarrow \Lambda\bar{\Lambda}$  and  $\Xi^-\bar{\Xi}^+$ .

Since the allowed open-charm decay channels of the  $Y(4220)$  include  $D\bar{D}$ ,  $D\bar{D}^* + c.c.$ ,  $D_s\bar{D}_s$  and  $D_s\bar{D}_s^* + c.c.$ , we should take into account the triangle loops composed of charmed mesons, which can be as the bridge to connect the initial  $Y(4220)$  and the  $\Lambda\bar{\Lambda}$  final state as shown in Fig. 1. If the intermediate charmed meson pair is  $D^{(*)}\bar{D}^{(*)}$ , the exchanged charmed baryon can be either  $\Xi_c$  or  $\Xi'_c$ , while, if the intermediate meson pair is  $D_s^{(*)}\bar{D}_s^{(*)}$ , the exchanged charmed baryon is  $\Lambda_c$ .

To evaluate these processes given in Fig. 1 at hadronic level, we first need construct the Lagrangians to describe the relevant interaction vertices. For the  $Y(4220)D^{(*)}\bar{D}^{(*)}$  interaction, we adopt the following form [41]

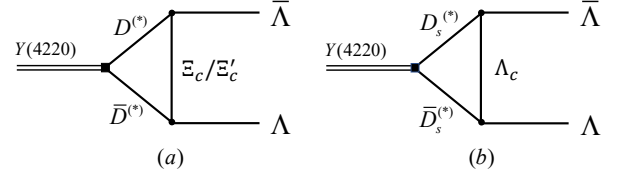


FIG. 1: The schematic diagrams for the  $Y(4220) \rightarrow \Lambda\bar{\Lambda}$  process of under hadronic loop mechanism.

$$\begin{aligned} \mathcal{L}_{\psi D^{(*)}\bar{D}^{(*)}} &= -ig_{\psi DD}\psi^\mu \left( \mathcal{D}^\dagger \overleftrightarrow{\partial}_\mu \mathcal{D} \right) \\ &+ g_{\psi DD^*} \epsilon^{\mu\nu\alpha\beta} \partial_\mu \psi_\nu \left( \mathcal{D}^\dagger \overleftrightarrow{\partial}_\alpha \mathcal{D}_\beta^* - \mathcal{D}_\beta^{*\dagger} \overleftrightarrow{\partial}_\alpha \mathcal{D} \right) \\ &+ ig_{\psi D^* \bar{D}^*} \psi^\mu \left( \partial^\nu \mathcal{D}_\mu^{*\dagger} \mathcal{D}_\nu^* - \mathcal{D}_\nu^{*\dagger} \partial^\nu \mathcal{D}_\mu^* + \mathcal{D}^{*\nu\dagger} \overleftrightarrow{\partial}_\mu \mathcal{D}_\nu^* \right). \end{aligned} \quad (1)$$

For depicting the interaction of  $B_c D^{(*)} \Lambda$ , where  $B_c$  denotes the charmed baryons, we use the following Lagrangian [42]

$$\begin{aligned} \mathcal{L}_{B_c D^{(*)} \Lambda} &= ig_{B_c D^{(*)} \Lambda} \bar{B}_c \gamma^5 D_{(s)} \Lambda \\ &+ \bar{B}_c \left( g_{B_c D^{(*)} \Lambda} \gamma^\mu + \frac{\kappa_{B_c D^{(*)} \Lambda}}{m_{B_c} + m_\Lambda} \sigma^{\mu\nu} \partial_\nu \right) D_{(s)\mu}^* \Lambda + h.c.. \end{aligned} \quad (2)$$

With the above preparation, we get the decay amplitudes of the  $Y(4220) \rightarrow \Lambda\bar{\Lambda}$  process corresponding to these diagrams in Fig. 1, the amplitudes corresponding to different charmed meson combinations are

$$\begin{aligned} \mathcal{M}^a &= i^3 \int \frac{d^4 q_3}{(2\pi)^4} (-ig_{\psi DD}) \epsilon_\psi^\mu (iq_{2\mu} - iq_{1\mu}) \\ &\times \bar{u}(p_2) \left( ig_{B_c D \Lambda} \gamma^5 \right) (\not{q}_3 + m_{B_c}) \left( ig_{B_c D \Lambda} \gamma^5 \right) v(p_1) \\ &\times \frac{1}{q_1^2 - m_D^2} \frac{1}{q_2^2 - m_D^2} \frac{1}{q_3^2 - m_{B_c}^2} \mathcal{F}^2(q_3^2), \end{aligned} \quad (3)$$

$$\begin{aligned} \mathcal{M}^b &= i^3 \int \frac{d^4 q_3}{(2\pi)^4} g_{\psi DD^*} \epsilon_\psi^\mu \epsilon_{\alpha\beta\lambda\mu} (iq_2^\alpha - iq_1^\alpha) (-ip^\lambda) \\ &\times \bar{u}(p_2) \left( ig_{B_c D \Lambda} \gamma^5 \right) (\not{q}_3 + m_{B_c}) \\ &\times \left( g_{B_c D^* \Lambda} \gamma^\rho - i \frac{\kappa_{B_c D^* \Lambda}}{m_{B_c} + m_\Lambda} \sigma^{\rho\nu} q_{2\nu} \right) v(p_1) \\ &\times \frac{1}{q_1^2 - m_D^2} \frac{-g_\rho^\beta + q_2^\beta q_{2\rho} / m_{D^*}^2}{q_2^2 - m_{D^*}^2} \frac{1}{q_3^2 - m_{B_c}^2} \mathcal{F}^2(q_3^2), \end{aligned} \quad (4)$$

$$\begin{aligned} \mathcal{M}^c &= i^3 \int \frac{d^4 q_3}{(2\pi)^4} g_{\psi DD^*} \epsilon_\psi^\mu \epsilon_{\alpha\beta\lambda\mu} (iq_1^\alpha - iq_2^\alpha) (-ip^\lambda) \\ &\times \bar{u}(p_2) \left( g_{B_c D^* \Lambda} \gamma^\rho - i \frac{\kappa_{B_c D^* \Lambda}}{m_{B_c} + m_\Lambda} \sigma^{\rho\nu} q_{1\nu} \right) \\ &\times (\not{q}_3 + m_{B_c}) \left( ig_{B_c D \Lambda} \gamma^5 \right) v(p_1) \\ &\times \frac{-g_\rho^\beta + q_2^\beta q_{2\rho} / m_{D^*}^2}{q_1^2 - m_{D^*}^2} \frac{1}{q_2^2 - m_D^2} \frac{1}{q_3^2 - m_{B_c}^2} \mathcal{F}^2(q_3^2), \end{aligned} \quad (5)$$

$$\begin{aligned}
\mathcal{M}^d = & i^3 \int \frac{d^4 q_3}{(2\pi)^4} i g_{\psi D^* D^*} \epsilon_{\psi}^{\mu} \left[ (i q_{2\mu} - i q_{1\mu}) g_{\alpha\nu} + i q_{1\alpha} g_{\mu\nu} \right. \\
& \left. - i q_{2\nu} g_{\mu\alpha} \right] \bar{u}(p_2) \left( g_{B_c D^* \Lambda} \gamma^\lambda - i \frac{\kappa_{B_c D^* \Lambda}}{m_{B_c} + m_\Lambda} \sigma^{\lambda\rho} q_{1\rho} \right) \\
& \times (q_3 + m_{B_c}) \left( g_{B_c D^* \Lambda} \gamma^\beta - i \frac{\kappa_{B_c D^* \Lambda}}{m_{B_c} + m_\Lambda} \sigma^{\beta\sigma} q_{2\sigma} \right) v(p_1) \\
& \times \frac{-g_{\lambda}^{\nu} + q_1^{\nu} q_{1\lambda} / m_{D^*}^2}{q_1^2 - m_{D^*}^2} \frac{-g_{\beta}^{\alpha} + q_2^{\alpha} q_{2\beta} / m_{D^*}^2}{q_2^2 - m_{D^*}^2} \frac{1}{q_3^2 - m_{B_c}^2} \mathcal{F}^2(q_3^2).
\end{aligned} \quad (6)$$

Here, as form factor,  $\mathcal{F}(q_3^2)$  is introduced to describe the off-shell effect of the exchanged charmed baryon in the rescattering process  $D^{(*)} \bar{D}^{(*)} \rightarrow \Lambda \bar{\Lambda}$ . In addition, introducing this form factor can avoid the divergence of the loop integral. In this work, we adopt the dipole form factor with expression

$$\mathcal{F}(q_3^2) = \left( \frac{m_E^2 - \Lambda^2}{q_3^2 - \Lambda^2} \right)^2, \quad \Lambda = m_E + \alpha \Lambda_{QCD}, \quad (7)$$

where  $m_E$  and  $q_3$  are the mass and four-momentum of the exchanged baryon, respectively.  $\Lambda_{QCD} = 220$  MeV, and  $\alpha$  denotes the phenomenological dimensionless parameter.

The total amplitude of the  $Y(4220) \rightarrow \Lambda \bar{\Lambda}$  process reads as

$$\mathcal{M}(Y(4220) \rightarrow \Lambda \bar{\Lambda}) = 2 \sum_{i=a,b,c,d} \left( \mathcal{M}_{\Xi_c}^i + \mathcal{M}_{\Xi_c'}^i \right) + \sum_{i=a,b,c,d} \mathcal{M}_{\Lambda_c}^i, \quad (8)$$

where the factor of 2 in front of  $\mathcal{M}_{\Xi_c}^i$  and  $\mathcal{M}_{\Xi_c'}^i$  comes from the summation over the isospin doublet ( $D^{0(*)}, D^{+(*)}$ ).

In the case of the  $Y(4220) \rightarrow \Xi^- \bar{\Xi}^+$  process, the intermediate charmed meson pairs can only be  $D^{+(*)} D^{-(*)}$  and  $D_s^{(*)} \bar{D}_s^{(*)}$ . For the  $D^{+(*)} D^{-(*)}$  intermediate state, the exchanged charmed baryon is  $\Omega_c$ . For the  $D_s^{(*)} \bar{D}_s^{(*)}$  intermediate state, the exchanged charmed baryon can be either  $\Xi_c$  or  $\Xi_c'$ . The allowed Feynman diagrams are showed in Fig. 2.

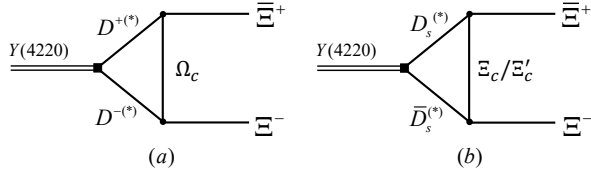


FIG. 2: The schematic diagrams of the  $Y(4220) \rightarrow \Xi^- \bar{\Xi}^+$  process induced by the hadronic loop mechanism.

To evaluate the diagrams given by Fig. 2, we need the effective Lagrangian of  $B_c D_{(s)}^{(*)} \Xi^-$  couplings besides the  $\mathcal{L}_{\psi D^{(*)} \bar{D}^{(*)}}$  given in Eq. (1), which has the same form as the Lagrangian of  $B_c D^{(*)} \Lambda$  interaction given in Eq. (2),

$$\begin{aligned}
\mathcal{L}_{B_c D_{(s)}^{(*)} \Xi} = & i g_{B_c D_{(s)} \Xi} \bar{B}_c \gamma^5 D_{(s)} \Xi \\
& + \bar{B}_c \left( g_{B_c D_{(s)}^* \Xi} \gamma^\mu + \frac{\kappa_{B_c D_{(s)}^* \Xi}}{m_{B_c} + m_\Xi} \sigma^{\mu\nu} \partial_\nu \right) D_{(s)\mu}^* \Xi + h.c..
\end{aligned} \quad (9)$$

Similar to the case of the  $Y(4220) \rightarrow \Lambda \bar{\Lambda}$  process, there are still four combinations of intermediate charmed meson pair as

seen in Fig. 2. They have the same forms as those in Eqs. (3)-(6). And the total amplitude of the  $Y(4220) \rightarrow \Xi^- \bar{\Xi}^+$  process reads as

$$\mathcal{M}(Y(4220) \rightarrow \Xi^- \bar{\Xi}^+) = \sum_{i=a,b,c,d} \left( \mathcal{M}_{\Omega_c}^i + \mathcal{M}_{\Xi_c}^i + \mathcal{M}_{\Xi_c'}^i \right). \quad (10)$$

With these amplitudes, the branching ratio of  $Y(4220) \rightarrow \Lambda \bar{\Lambda} / \Xi^- \bar{\Xi}^+$  can be calculated by

$$\mathcal{B} = \frac{1}{3} \frac{1}{8\pi} \frac{|P_{\Lambda/\Xi^-}^{cm}|}{m_Y^2 \Gamma_Y} \sum_{pol.} \left| \mathcal{M}(Y(4220) \rightarrow \Lambda \bar{\Lambda} / \Xi^- \bar{\Xi}^+) \right|^2, \quad (11)$$

where the factor of 1/3 is due to spin average over an initial charmonium state.

## B. The EMFFs of $\Lambda$ and $\Xi^-$ at $\sqrt{s} = m_{Y(4220)}$

As mentioned in the introduction, the time-like EMFFs at specific resonance point reflect the complete amplitude of the resonance decay. However, the decay branching ratio only utilize the module of the amplitude. So in this section, we illustrate the relation of the EMFFs of  $\Lambda$  and  $\Xi^-$  at  $\sqrt{s} = m_{Y(4220)}$  with the amplitudes of the  $Y(4220) \rightarrow \Lambda \bar{\Lambda}$  and  $\Xi^- \bar{\Xi}^+$  processes.

The photon interacting with baryon and anti-baryon is absorbed into the vertex  $\gamma B \bar{B}$ , which can be described by the so-called Sachs EMFFs  $G_E$  and  $G_M$  [43]. In terms of  $G_E$  and  $G_M$ , the  $\gamma B \bar{B}$  vertex can be expressed as

$$-ie\Gamma^\mu = -ie\bar{u}(p_2) \left( G_M \gamma^\mu - \frac{2m_\Lambda}{Q^2} (G_M - G_E) Q^\mu \right) v(p_1), \quad (12)$$

where  $Q = p_2 - p_1$ ,  $G_E$  and  $G_M$  are the electric and magnetic form factors, respectively. The form factors  $G_E$  and  $G_M$  are analytical functions of the four-momentum transfer squared  $q^2$ , analytic in the  $q^2$ -complex plane with a branch cut along the positive real axis because of possible hadronic channels coupled with the virtual photon and the  $B \bar{B}$  state. In the space-like region  $q^2 < 0$ , both  $G_E$  and  $G_M$  are real values which can be measured by the scattering process  $e^- B \rightarrow e^- B$ . In the time-like region  $q^2 = s > (2m_B)^2$ , the form factors are complex numbers because of the hadronic channels coupled with both of photon and  $B \bar{B}$  state<sup>1</sup>.

In the time-like region, the  $G_E$  and  $G_M$  can be extracted from the  $e^+ e^-$  annihilation processes  $e^+ e^- \rightarrow B \bar{B}$ . Especially, the relative phase  $\Delta\Phi = \arg(G_E/G_M)$  is related to the polarization of the produced baryon or antibaryon. Directly measuring the polarization of a baryon is not realistic. An alternate approach to obtain the polarization of a hyperon is through the angular distribution of the subsequent decay of a hyperon like  $\Xi \rightarrow \Lambda \pi$  and  $\Lambda \rightarrow p \pi$ . Recently, several measurements of the complete EMFFs of  $\Lambda$  and  $\Xi^-$  have been done by BESIII. The

<sup>1</sup> Actually, we are discussing the region  $q^2 + i\epsilon$  since the physical scattering amplitudes are evaluated above the branch cut.

module and relative phase of the EMFFs of  $\Lambda$  were given at  $\sqrt{s} = m_{J/\psi}$  [22] and  $\sqrt{s} = 2.396$  GeV [25]. The EMFFs of  $\Xi^-$  were measured at  $\sqrt{s} = m_{J/\psi}$  [26].

In the region of baryon production near mass threshold of the baryon pair, the behaviors of EMFFs become strange and near threshold enhancement effect was observed. For example, the BESIII Collaboration observed an enhancement of the cross section of  $e^+e^- \rightarrow \Lambda\bar{\Lambda}$  just above the  $\Lambda\bar{\Lambda}$  mass threshold [44]. Also, similar behavior existing in  $e^+e^- \rightarrow \Lambda_c\bar{\Lambda}_c$  was observed near the  $\Lambda_c\bar{\Lambda}_c$  mass threshold [45]. However, in the  $q^2$  region away from the production threshold, the contribution of the intermediate resonance dominates the cross section at the specific resonance energy point such as the process  $e^+e^- \rightarrow \Lambda\bar{\Lambda}$  at  $\sqrt{s} = m_{J/\psi}$  and  $\sqrt{s} = m_{\psi'}$ . In this work, we focus on the EMFFs of  $\Lambda$  and  $\Xi^-$  at  $\sqrt{s} = m_{Y(4220)}$ . Since the mass of the  $Y(4220)$  is far from the  $\Lambda\bar{\Lambda}$  and  $\Xi^-\bar{\Xi}^+$  mass threshold, we can avoid the complicated situation caused by the threshold.

At  $\sqrt{s} = m_{Y(4220)}$ , the process we considered is actually  $e^+e^- \rightarrow \gamma^* \rightarrow Y(4220) \rightarrow \Lambda\bar{\Lambda}/\Xi^-\bar{\Xi}^+$  due to the observed  $Y(4220)$ . The  $\gamma^*\Lambda\bar{\Lambda}$  and  $\gamma^*\Xi^-\bar{\Xi}^+$  vertices are dominated by the hadronic intermediate states, where the triangle loops composed of charmed mesons may have connection with both the  $Y(4220)$  and the final state  $\Lambda\bar{\Lambda}/\Xi^-\bar{\Xi}^+$  (see Fig. 3). Then EMFFs of  $\Lambda\bar{\Lambda}$  and  $\Xi^-\bar{\Xi}^+$  can reflect the information of these hadronic loops. The loop integral has both real and imaginary parts corresponding to the complex EMFFs exactly.

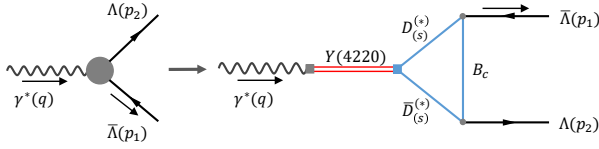


FIG. 3:  $\gamma \rightarrow \Lambda\bar{\Lambda}$  under the hadronic loop mechanism. Here, energy point is fixed to be  $\sqrt{s} = m_{Y(4220)}$  and  $B_c$  denotes these allowed charmed baryons.

The amplitudes of these Feynman diagrams in Fig. 3 are almost the same as those in the previous section, the only difference is that we need to couple the vector  $Y$  state with a virtual photon. This is described by the Lagrangian

$$\mathcal{L}_{\gamma Y} = \frac{-em_Y^2}{f_Y} Y_\mu A^\mu. \quad (13)$$

Writing out the amplitude of  $Y(4220) \rightarrow \Lambda\bar{\Lambda}/\Xi^-\bar{\Xi}^+$  in the form  $\mathcal{M} = \epsilon_\mu^Y \mathcal{M}_\mu^Y$ , then the  $\gamma^* B\bar{B}$  vertex is further expressed as

$$\mathcal{M}_{\gamma^* B\bar{B}}^\mu = -\frac{em_Y^2}{f_Y} \frac{-g^{\mu\kappa} + q^\mu q^\kappa/m_Y^2}{q^2 - m_Y^2 + im_Y\Gamma_Y} \mathcal{M}_\kappa^Y. \quad (14)$$

After evaluating the loop integral in the amplitude, this vertex can be reduced to the form of Eq. (12), from which we can get the result of the form factors  $G_E$  and  $G_M$ .

### III. NUMERICAL RESULTS AND DISCUSSIONS

To evaluate the branching ratios of the  $Y(4220) \rightarrow \Lambda\bar{\Lambda}$  and  $\Xi^-\bar{\Xi}^+$  processes, we need to fix the coupling constants in the effective Lagrangians. The coupling constants in Eq. (1) can be extracted by theoretical result of partial widths of the  $Y(4220)$  from Ref. [19], which are collected in Table I. The coupling constants of  $B_c D^{(*)}\Lambda$  and  $B_c D^{(*)}\Xi$  interactions are obtained from the couplings of  $\Lambda_c DN$  and  $\Sigma_c DN$  by applying SU(3) symmetry. Here, we use the  $\Lambda_c DN$  and  $\Sigma_c DN$  coupling constants obtained from the results of QCD light-cone sum rules as [42]

$$\begin{aligned} g_{\Lambda_c DN} &= 13.8, & g_{\Sigma_c DN} &= 1.3, \\ g_{\Lambda_c D^* N} &= -7.9, & g_{\Sigma_c D^* N} &= 1.0, \\ \kappa_{\Lambda_c D^* N} &= 4.7, & \kappa_{\Sigma_c D^* N} &= 2.1. \end{aligned}$$

And then, with SU(3) symmetry, the various couplings needed can be obtained by the following relations

$$\begin{aligned} \sqrt{\frac{3}{2}} g_{\Lambda_c D_s^{(*)}\Lambda} &= \sqrt{6} g_{\Xi_c D^{(*)}\Lambda} = g_{\Xi_c D_s^{(*)}\Xi} = g_{\Lambda_c D^{(*)}N}, \\ \sqrt{\frac{2}{3}} g_{\Xi_c D^{(*)}\Lambda} &= \frac{1}{\sqrt{2}} g_{\Omega_c D^{(*)}\Xi} = g_{\Xi_c D_s^{(*)}\Xi} = g_{\Sigma_c D^{(*)}N}, \end{aligned}$$

where we omit possible minus signs in various coupling constants because they always appear twice in the amplitudes.

The calculated branching ratios of the  $Y(4220) \rightarrow \Lambda\bar{\Lambda}$  and  $\Xi^-\bar{\Xi}^+$  processes are shown in Fig. 5 and Fig. 6, respectively. Given the possible signals of the  $Y(4220)$  in  $e^+e^- \rightarrow \Lambda\bar{\Lambda}$  [23] and  $e^+e^- \rightarrow \Xi^-\bar{\Xi}^+$  [24] processes, we try to extract the branching ratios of the  $Y(4220) \rightarrow \Lambda\bar{\Lambda}$  and  $\Xi^-\bar{\Xi}^+$  processes from the experimental data by using the phase space corrected Breit-Wigner distribution

$$\mathcal{M}_R(Y) = \frac{\sqrt{12\pi\Gamma_Y^{e^+e^-} \mathcal{B}(Y \rightarrow \Lambda\bar{\Lambda}/\Xi^-\bar{\Xi}^+) \Gamma_Y}}{s - m_Y^2 + im_Y\Gamma_Y} \sqrt{\frac{\Phi(s)}{\Phi(m_Y^2)}}, \quad (15)$$

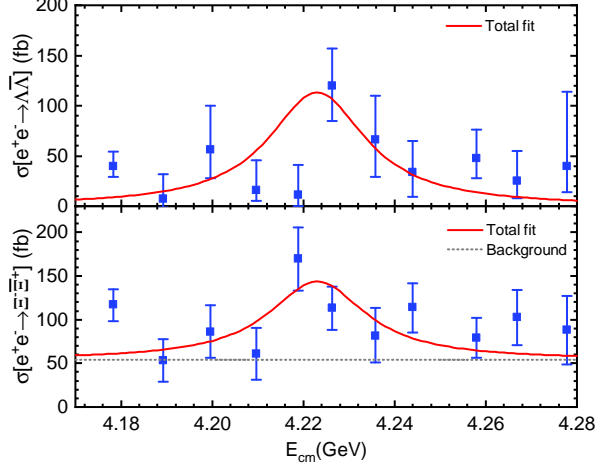
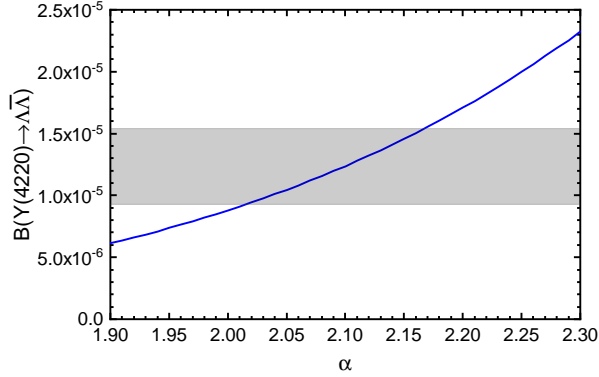
where  $\Phi(s)$  denotes the two-body phase space. The mass, width, and dilepton width of the  $Y(4220)$  are taken from the calculated values in Ref. [19], *i.e.*,  $m_{Y(4220)} = 4220$  MeV,  $\Gamma_{Y(4220)} = 26$  MeV, and  $\Gamma_Y^{e^+e^-} = 0.29$  keV. The results of these simple fits are shown in Fig. 4, from which we obtain the branching ratios as

$$\begin{aligned} \mathcal{B}(Y(4220) \rightarrow \Lambda\bar{\Lambda}) &= (12.35 \pm 3.06) \times 10^{-6}, \\ \mathcal{B}(Y(4220) \rightarrow \Xi^-\bar{\Xi}^+) &= (9.77 \pm 2.19) \times 10^{-6}. \end{aligned} \quad (16)$$

These extracted branching ratios are shown in Fig. 5 and Fig. 6 as shadowed regions. The calculated branching ratios of these two decay channels are shown as blue curves, which dependent on the cutoff parameter  $\alpha$  appeared in the form factor. We find that the extracted branching ratio of the  $Y(4220) \rightarrow \Lambda\bar{\Lambda}$  process in Eq. (16) can be reproduced well when  $\alpha$  is taken as the 2.01 ~ 2.17 range. And, in our theoretical framework, we also reproduce the extracted branching

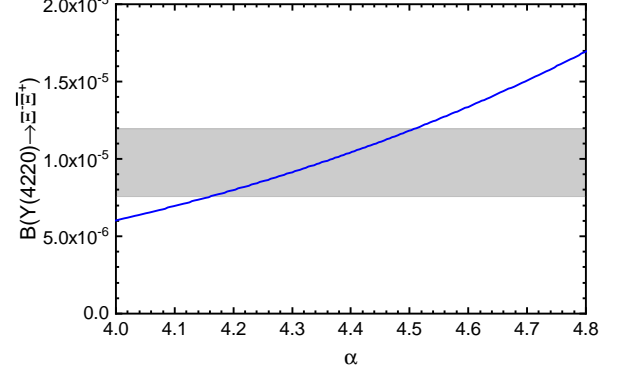
TABLE I: Partial widths of the open-charm decay of the  $Y(4220)$  [19] and the obtained coupling constants.

Channel	$DD$	$DD^*$	$D^*D^*$	$D_sD_s$	$D_sD_s^*$
Partial width (MeV)	3.29	0.723	21.8	0.144	0.0486
Coupling constant	0.765	$0.054 \text{ GeV}^{-1}$	1.320	0.233	$0.027 \text{ GeV}^{-1}$

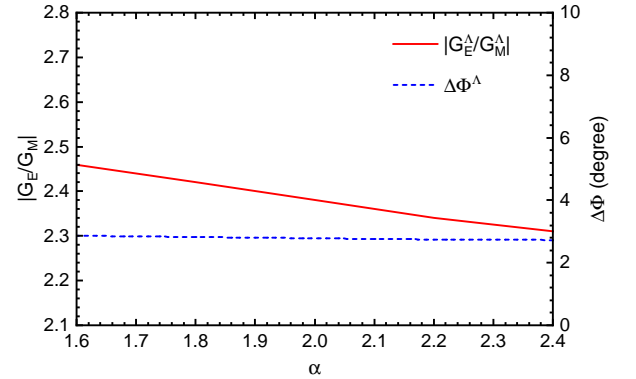
FIG. 4: The possible signals of the  $Y(4220)$  existing in the  $e^+e^- \rightarrow \Lambda\bar{\Lambda}$  [23] and  $e^+e^- \rightarrow \Xi^-\bar{\Xi}^+$  [24] channel. Here, for fitting the  $e^+e^- \rightarrow \Xi^-\bar{\Xi}^+$  data, a constant background is used.FIG. 5: The  $\alpha$  dependence of the branching ratio of  $Y(4220) \rightarrow \Lambda\bar{\Lambda}$ . Here, grey band is the extracted branching ratio from the experiment data.

ratio of the  $Y(4220) \rightarrow \Xi^-\bar{\Xi}^+$  process when taking  $\alpha$  to be  $4.17 \sim 4.52$ .

In Fig. 7 and Fig. 8, we show the obtained EMFFs of  $\Lambda$  and  $\Xi^-$ , respectively, from which we can see that the behavior of the  $|G_E/G_M|$  and  $\Delta\Phi$  for  $\Lambda$  and  $\Xi^-$  are quite different. Here, the  $|G_E/G_M|$  of  $\Lambda$  is about 2.4 while that of  $\Xi^-$  is around 0.4. In addition, the  $\Delta\Phi$  of  $\Lambda$  has small value, while the  $\Delta\Phi$  of  $\Xi^-$  has a much larger absolute value, and has a minus sign. For these two processes, the  $|G_E/G_M|$  and  $\Delta\Phi$  have weak dependence on  $\alpha$ , where the predicted ratios of EMFFs are stable. The results of EMFFs of  $\Lambda$  and  $\Xi^-$  when taking typical values  $\alpha_\Lambda = 2.10$  and  $\alpha_{\Xi^-} = 4.34$  are collected in Table II. We

FIG. 6: The  $\alpha$  dependence of the branching ratio of  $Y(4220) \rightarrow \Xi^-\bar{\Xi}^+$ . Here, the grey band is the extracted branching ratio from the experiment data.

suggest future experiment like BESIII and BelleII to perform the measurement of these EMFFs, by which the charmonia assignment to the  $Y(4220)$  can be further tested.

FIG. 7: The  $\alpha$  dependence of the  $|G_E/G_M|$  and  $\Delta\Phi$  of  $\Lambda$  at  $\sqrt{s} = m_{Y(4220)}$ .TABLE II: The predicted ratios of EMFFs of  $\Lambda$  and  $\Xi^-$  at  $\sqrt{s} = m_{Y(4220)}$ .

Form factor	$ G_E^\Lambda/G_M^\Lambda $	$\Delta\Phi^\Lambda$	$ G_E^{\Xi^-}/G_M^{\Xi^-} $	$\Delta\Phi^{\Xi^-}$
Value	2.36	$2.74^\circ$	0.40	$-115.60^\circ$

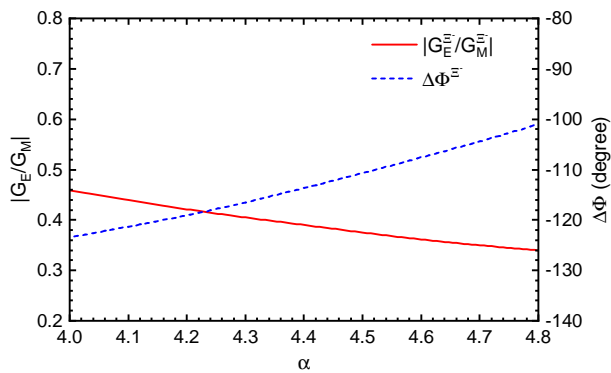


FIG. 8: The  $\alpha$  dependence of the  $|G_E^-/G_M^-|$  and  $\Delta\Phi^-$  of  $\Xi^-$  at  $\sqrt{s} = m_{Y(4220)}$ .

#### IV. DISCUSSION AND CONCLUSION

With the accumulation of experimental data, charmoniumlike state  $Y(4220)$  was observed by BESIII in  $e^+e^- \rightarrow J/\psi\pi^+\pi^-$  [20],  $e^+e^- \rightarrow h_c\pi^+\pi^-$  [21],  $e^+e^- \rightarrow \chi_{c0}\omega$  [16], and  $e^+e^- \rightarrow \psi(3686)\pi^+\pi^-$  [17], which is consistent with the predicted vector charmonium state around 4.2 GeV [5]. As indicated by the recent work, the  $Y(4220)$  can be assigned to be the mixture of the  $\psi(4S)$  and  $\psi(3D)$  charmonium states [19]. What is more important is that the  $Y(4220)$  may play the role of scaling point when constructing the  $J/\psi$  family.

In fact, the hidden-charm decay is only one mode of these allowed decays of the  $Y(4220)$  under the vector charmonium assignment to the  $Y(4220)$ . Later, the BESIII observation of an enhancement around 4.2 GeV in the  $e^+e^- \rightarrow \pi^+D^0D^{*-}$  enforces the above conclusion of decoding the  $Y(4260)$  as charmonium [18].

If checking the decay behaviors of these established charmonia like  $J/\psi$ ,  $\psi(3686)$  and  $\psi(3770)$ , we find their abundant decay modes [46]. Besides hidden-charm and open-charm decays, there exist the decays into light hadrons for charmonium.

Inspired by the above situation, we propose to study the

$Y(4220)$  decays into  $\Lambda\bar{\Lambda}$  and  $\Xi^-\bar{\Xi}^+$ , which is also due to the experimental potential of analyzing these decays [23, 24]. We notice the possible evidence of the  $Y(4220)$  existing in the reported data of  $e^+e^-$  annihilation into  $\Lambda\bar{\Lambda}$  and  $\Xi^-\bar{\Xi}^+$  channels. We may roughly extract the branching ratios of these two decays for further study, which are of the order of magnitude  $10^{-5}$ .

Assigning the  $Y(4220)$  as a charmonium state, we adopt the hadronic loop mechanism to evaluate these two processes and find that the obtained branching ratios of  $Y(4220) \rightarrow \Lambda\bar{\Lambda}$  and  $\Xi^-\bar{\Xi}^+$  can reproduce the extracted value, which may enforce the  $Y(4220)$  as a charmonium state again. By taking this opportunity, we strongly suggest our experimental colleague to focus on the precise measurement of  $e^+e^- \rightarrow \Lambda\bar{\Lambda}$  and  $\Xi^-\bar{\Xi}^+$ , especially identifying the  $Y(4220)$ .

After reproducing the extracted branching ratios, we further predict the EMFFs of  $\Lambda$  and  $\Xi^-$  at  $\sqrt{s} = m_{Y(4220)}$ . The  $|G_E^\Lambda/G_M^\Lambda|$  and  $\Delta\Phi^\Lambda$  are predicted to be 2.36 and  $2.74^\circ$ , respectively. And, the  $|G_E^{\Xi^-}/G_M^{\Xi^-}|$  and  $\Delta\Phi^{\Xi^-}$  are predicted to be 0.40 and  $-115.60^\circ$ , respectively. These predictions on EMFFs can be accessible at future experiment like BESIII and BelleII.

Very recently, BESIII reported the measurement of EMFFs at  $\sqrt{s} = 3.773$  GeV [47] which is in the vicinity  $\psi(3770)$  peak. The measurement of EMFFs at  $Y(4220)$  point will be an interesting topic in the near future. We hope that future experiments like BESIII and BelleII can seriously focus on this issue with higher precision.

#### Acknowledgments

This work is supported by the China National Funds for Distinguished Young Scientists under Grant No. 11825503, National Key Research and Development Program of China under Contract No. 2020YFA0406400, the 111 Project under Grant No. B20063, the National Natural Science Foundation of China under Grant No. 12047501, and by the Fundamental Research Funds for the Central Universities.

- 
- [1] J. J. Aubert *et al.* (E598 Collaboration), Experimental Observation of a Heavy Particle  $J$ , *Phys. Rev. Lett.* **33**, 1404 (1974).  
[2] J. E. Augustin *et al.* (SLAC-SP-017 Collaboration), Discovery of a Narrow Resonance in  $e^+e^-$  Annihilation, *Phys. Rev. Lett.* **33**, 1406 (1974).  
[3] Y. R. Liu, H. X. Chen, W. Chen, X. Liu, and S. L. Zhu, Pentaquark and Tetraquark states, *Prog. Part. Nucl. Phys.* **107**, 237 (2019).  
[4] N. Brambilla, S. Eidelman, C. Hanhart, A. Nefediev, C. P. Shen, C. E. Thomas, A. Vairo, and C. Z. Yuan, The XYZ states: experimental and theoretical status and perspectives, *Phys. Rept.* **873**, 1 (2020).  
[5] L. P. He, D. Y. Chen, X. Liu, and T. Matsuki, Prediction of a missing higher charmonium around 4.26 GeV in  $J/\psi$  family, *Eur. Phys. J. C* **74**, 3208 (2014).  
[6] B. Q. Li and K. T. Chao, Higher Charmonia and X, Y, Z states with Screened Potential, *Phys. Rev. D* **79**, 094004 (2009).  
[7] B. Q. Li and K. T. Chao, Higher Charmonia and X, Y, Z states with Screened Potential, *Phys. Rev. D* **79**, 094004 (2009).  
[8] C. Z. Yuan, Evidence for resonant structures in  $e^+e^- \rightarrow \pi^+\pi^-h_c$ , *Chin. Phys. C* **38**, 043001 (2014).  
[9] M. Ablikim *et al.* (BESIII Collaboration), Observation of a Charged Charmoniumlike Structure  $Z_c(4020)$  and Search for the  $Z_c(3900)$  in  $e^+e^- \rightarrow \pi^+\pi^-h_c$ , *Phys. Rev. Lett.* **111**, 242001 (2013).  
[10] Z. Q. Liu *et al.* (Belle Collaboration), Study of  $e^+e^- \rightarrow \pi^+\pi^-J/\psi$  and Observation of a Charged Charmoniumlike State at Belle, *Phys. Rev. Lett.* **110**, 252002 (2013).  
[11] M. Ablikim *et al.* (BESIII Collaboration), Study of  $e^+e^- \rightarrow \omega\chi_{cJ}$  at center-of-mass energies from 4.21 to 4.42 GeV, *Phys. Rev. Lett.* **114**, 092003 (2015).  
[12] D. Y. Chen, X. Liu, and T. Matsuki, Observation of  $e^+e^- \rightarrow$

- $\chi_{c0}\omega$  and missing higher charmonium  $\psi(4S)$ , *Phys. Rev. D* **91**, 094023 (2015).
- [13] D. Y. Chen, X. Liu, and T. Matsuki, Search for missing  $\psi(4S)$  in the  $e^+e^- \rightarrow \pi^+\pi^-\psi(2S)$  process, *Phys. Rev. D* **93**, 034028 (2016)
- [14] X. L. Wang *et al.* (Belle Collaboration), Measurement of  $e^+e^- \rightarrow \pi^+\pi^-\psi(2S)$  via Initial State Radiation at Belle, *Phys. Rev. D* **91**, 112007 (2015).
- [15] X. L. Wang *et al.* (Belle Collaboration), Measurement of  $e^+e^- \rightarrow \pi^+\pi^-\psi(2S)$  via Initial State Radiation at Belle, *Phys. Rev. D* **91**, 112007 (2015).
- [16] M. Ablikim *et al.* (BESIII Collaboration), Study of  $e^+e^- \rightarrow \omega\chi_{cJ}$  at center-of-mass energies from 4.21 to 4.42 GeV, *Phys. Rev. Lett.* **114**, 092003 (2015).
- [17] M. Ablikim *et al.* (BESIII Collaboration), Measurement of  $e^+e^- \rightarrow \pi^+\pi^-\psi(3686)$  from 4.008 to 4.600 GeV and observation of a charged structure in the  $\pi^\pm\psi(3686)$  mass spectrum, *Phys. Rev. D* **96**, 032004 (2017); **99**, 019903(E) (2019).
- [18] M. Ablikim *et al.* (BESIII Collaboration), Evidence of a resonant structure in the  $e^+e^- \rightarrow \pi^+D^0D^{*-}$  cross section between 4.05 and 4.60 GeV, *Phys. Rev. Lett.* **122**, 102002 (2019).
- [19] J. Z. Wang, D. Y. Chen, X. Liu, and T. Matsuki, Constructing  $J/\psi$  family with updated data of charmoniumlike  $Y$  states, *Phys. Rev. D* **99**, 114003 (2019).
- [20] M. Ablikim *et al.* (BESIII Collaboration), Precise measurement of the  $e^+e^- \rightarrow \pi^+\pi^-J/\psi$  cross section at center-of-mass energies from 3.77 to 4.60 GeV, *Phys. Rev. Lett.* **118**, 092001 (2017).
- [21] M. Ablikim *et al.* (BESIII Collaboration), Evidence of Two Resonant Structures in  $e^+e^- \rightarrow \pi^+\pi^-h_c$ , *Phys. Rev. Lett.* **118**, 092002 (2017).
- [22] M. Ablikim *et al.* (BESIII Collaboration), Polarization and Entanglement in Baryon-Antibaryon Pair Production in Electron-Positron Annihilation, *Nature Phys.* **15**, 631 (2019).
- [23] M. Ablikim *et al.* (BESIII Collaboration), Measurement of the Cross Section for  $e^+e^- \rightarrow \Lambda\bar{\Lambda}$  and Observation of the Decay  $\psi(3770) \rightarrow \Lambda\bar{\Lambda}$ , [arXiv: 2108.02410](https://arxiv.org/abs/2108.02410).
- [24] M. Ablikim *et al.* (BESIII Collaboration), Measurement of the cross section for  $e^+e^- \rightarrow \Xi^-\bar{\Xi}^+$  and observation of an excited  $\Xi$  baryon, *Phys. Rev. Lett.* **124**, 032002 (2020).
- [25] M. Ablikim *et al.* (BESIII Collaboration), Complete Measurement of the  $\Lambda$  Electromagnetic Form Factors, *Phys. Rev. Lett.* **123**, 122003 (2019).
- [26] M. Ablikim *et al.* (BESIII Collaboration), Weak phases and CP-symmetry tests in sequential decays of entangled double-strange baryons, [arXiv: 2105.11155](https://arxiv.org/abs/2105.11155).
- [27] M. Ablikim *et al.* (BESIII Collaboration),  $\Sigma^+$  and  $\bar{\Sigma}^-$  polarization in the  $J/\psi$  and  $\psi(3686)$  decays, *Phys. Rev. Lett.* **125**, 052004 (2020).
- [28] X. Liu, X. Q. Zeng, and X. Q. Li, Study on contributions of hadronic loops to decays of  $J/\psi \rightarrow \text{vector} + \text{pseudoscalar mesons}$ , *Phys. Rev. D* **74**, 074003 (2006).
- [29] X. Liu, B. Zhang, and X. Q. Li, The Puzzle of excessive non- $DD$  component of the inclusive  $\psi(3770)$  decay and the long-distant contribution, *Phys. Lett. B* **675**, 441 (2009).
- [30] Y. J. Zhang, G. Li, and Q. Zhao, Further understanding of the non- $DD$  decays of  $\psi(3770)$ , *Phys. Rev. Lett.* **102**, 172001 (2009).
- [31] C. Meng and K. T. Chao, Scalar resonance contributions to the dipion transition rates of  $\Upsilon(4S, 5S)$  in the rescattering model, *Phys. Rev. D* **77**, 074003 (2008).
- [32] C. Meng and K. T. Chao, Peak shifts due to  $B^{(*)} - \bar{B}^{(*)}$  rescattering in  $\Upsilon(5S)$  dipion transitions, *Phys. Rev. D* **78**, 034022 (2008).
- [33] C. Meng and K. T. Chao,  $\Upsilon(4S, 5S) \rightarrow \Upsilon(1S)\eta$  transitions in the rescattering model and the new BABAR measurement, *Phys. Rev. D* **78**, 074001 (2008).
- [34] D. Y. Chen, J. He, X. Q. Li, and X. Liu, Dipion invariant mass distribution of the anomalous  $\Upsilon(1S)\pi^+\pi^-$  and  $\Upsilon(2S)\pi^+\pi^-$  production near the peak of  $\Upsilon(10860)$ , *Phys. Rev. D* **84**, 074006 (2011).
- [35] D. Y. Chen, X. Liu, and S. L. Zhu, Charged bottomonium-like states  $Z_b(10610)$  and  $Z_b(10650)$  and the  $\Upsilon(5S) \rightarrow \Upsilon(2S)\pi^+\pi^-$  decay, *Phys. Rev. D* **84**, 074016 (2011).
- [36] D. Y. Chen and X. Liu,  $Z_b(10610)$  and  $Z_b(10650)$  structures produced by the initial single pion emission in the  $\Upsilon(5S)$  decays, *Phys. Rev. D* **84**, 094003 (2011).
- [37] D. Y. Chen, X. Liu, and T. Matsuki, Explaining the anomalous  $\Upsilon(5S) \rightarrow \chi_{bJ}\omega$  decays through the hadronic loop effect, *Phys. Rev. D* **90**, 034019 (2014).
- [38] B. Wang, X. Liu, and D. Y. Chen, Prediction of anomalous  $\Upsilon(5S) \rightarrow \Upsilon(1^3D_J)\eta$  transitions, *Phys. Rev. D* **94**, 094039 (2016).
- [39] Q. Huang, B. Wang, X. Liu, D. Y. Chen, and T. Matsuki, Exploring the  $\Upsilon(6S) \rightarrow \chi_{bJ}\phi$  and  $\Upsilon(6S) \rightarrow \chi_{bJ}\omega$  hidden-bottom hadronic transitions, *Eur. Phys. J. C* **77**, 165 (2017).
- [40] Q. Huang, X. Liu, and T. Matsuki, Proposal of searching for the  $\Upsilon(6S)$  hadronic decays into  $\Upsilon(nS)$  plus  $\eta^{(\prime)}$ , *Phys. Rev. D* **98**, 054008 (2018).
- [41] Q. Huang, H. Xu, X. Liu, and T. Matsuki, Potential observation of the  $\Upsilon(6S) \rightarrow \Upsilon(1^3D_J)\eta$  transitions at Belle II, *Phys. Rev. D* **97**, 094018 (2018).
- [42] A. Khodjamirian, C. Klein, T. Mannel, and Y. M. Wang, Form Factors and Strong Couplings of Heavy Baryons from QCD Light-Cone Sum Rules, *JHEP* **09**, 106 (2011).
- [43] F. J. Ernst, R. G. Sachs and K. C. Wali, Electromagnetic form factors of the nucleon, *Phys. Rev.* **119**, 1105 (1960).
- [44] M. Ablikim *et al.* (BESIII Collaboration), Observation of a cross-section enhancement near mass threshold in  $e^+e^- \rightarrow \Lambda\bar{\Lambda}$ , *Phys. Rev. D* **97**, 032013 (2018).
- [45] M. Ablikim *et al.* (BESIII Collaboration), Precision measurement of the  $e^+e^- \rightarrow \Lambda_c^+\bar{\Lambda}_c^-$  cross section near threshold, *Phys. Rev. Lett.* **120**, 132001 (2018).
- [46] P. A. Zyla *et al.* (Particle Data Group Collaboration), Review of Particle Physics, *Porg. Theor. Exp. Phys.* **2020**, 083C01 (2020).
- [47] M. Ablikim *et al.* (BESIII Collaboration), Measurement of  $\Lambda$  baryon polarization in  $e^+e^- \rightarrow \Lambda\bar{\Lambda}$  at  $\sqrt{s} = 3.773$  GeV, [arXiv: 2111.11742](https://arxiv.org/abs/2111.11742).